Zipper Mechanism of Nanotube Fusion: Theory and Experiment

Mina Yoon,[1] Seungwu Han,[2,*] Gunn Kim,[3] Sang Bong Lee,[3] Savas Berber,[1] Eiji Osawa,[4] Jisoon Ihm,[3]
Mauricio Terrones,[5] Florian Banhart,[6] Jean-Christophe Charlier,[7] Nicole Grobert,[8] Humberto Terrones,[5]
Pulickel M. Ajayan,[9] and David Tománek[1,†]

[1]*Department of Physics and Astronomy, Michigan State University, East Lansing, Michigan 48824-2320, USA*
[2]*Princeton Materials Institute, Princeton University, Princeton, New Jersey 08544, USA*
[3]*School of Physics, Seoul National University, Seoul 151-747, Korea*
[4]*NanoCarbon Research Institute Limited, Chosei-mura, Chosei-gun, Chiba 2994395, Japan*
[5]*Advanced Materials Department, IPICyT, Avenida Venustiano Carranza 2425-A, 78210 San Luis Potosí, SLP, México*
[6]*Institut für Physikalische Chemie, Universität Mainz, Welderweg 11, 55099 Mainz, Germany*
[7]*Université Catholique de Louvain, PCPM&CERMIN, B-1348 Louvain-la-Neuve, Belgium*
[8]*Max-Planck-Institut für Metallforschung, Heisenbergstrasse 3, D-70569 Stuttgart, Germany*
[9]*Department of Materials Science & Engineering, Rensselaer Polytechnic Institute, Troy, New York 12180-3590, USA*
(Received 12 August 2003; published 19 February 2004)

We propose a new microscopic mechanism to explain the unusually fast fusion process of carbon nanotubes. We identify the detailed pathway for two adjacent (5,5) nanotubes to gradually merge into a (10,10) tube, and characterize the transition states. The propagation of the fused region is energetically favorable and proceeds in a morphology reminiscent of a Y junction via a zipper mechanism, involving only Stone-Wales bond rearrangements with low activation barriers. The zipper mechanism of fusion is supported by a time series of high-resolution transmission electron microscopy observations.

Fullerenes [1] and nanotubes [2] are likely candidates for hierarchical self-assembly of nanoscale devices with complex geometries. As potential building blocks of nanotechnology, they are unusually stable and inert, suggesting that they should remain structurally stable once synthesized. Consequently, it remains an unsolved problem, why nanotubes and other sp^2-bonded carbon nanostructures are observed to fuse so efficiently [3,4]. Especially puzzling appears the high speed of these structural transformations even at relatively low temperatures, implying a process with a very low activation barrier. A detailed understanding of this process may open a route to directing the assembly of more complex functional nanostructures.

Fusion pathways that have been discussed thus far involve vacancy generation to establish a local connection between tubes and to propagate this connection as the tubes merge [3]. Yet the high energy cost associated with bond breaking is inconsistent with the high speed of the fusion process following the formation of the initial connection. Here, we propose a microscopic zipper mechanism that involves only bond rotations instead of bond breaking to speed up the merging process in partially fused tubes. Our findings offer a new insight into the observed fast coalescence of single-walled carbon nanotubes (SWNTs) under *in situ* irradiation and heating in a high-resolution transmission electron microscope (HRTEM) [3].

The Y-junction structure used in our study of nanotube fusion, resembling the shape of pants, is shown in Fig. 1(a). This generic structure forms when, in the presence of atomic defects, a local connection is established between adjacent nanotubes. The structure consists of a (10, 10) nanotube section representing the waist and two (5, 5) nanotubes representing the legs, and could be created by bond rearrangement during electron irradiation under experimental conditions. The bonding topology in the defective region, where the tubes are connected, is vacancy free, which has never been considered before. The junction region shows negative Gaussian curvature. It contains higher polygons, including heptagons or octagons, inserted in the sp^2-bonded hexagonal network forming the tubes. In this Letter, we show that a continuous fusion process is possible in this geometry. In view of the instability associated with the insertion of high polygons, we focused on Y-junction geometries containing only heptagons and octagons in the hexagon network.

Our main objective is to find out if it is possible to advance the axial position of the defect region and thus to merge the tubes by means of bond rearrangements only, similar to a zipper that reversibly connects or disconnects two pieces of fabric. In order to find all acceptable pathways leading to coalescence, a nontrivial topological problem, we use a graphical search program that was initially developed to study the fusion of fullerenes [5]. Since the initial steps of the local bridge formation between nanotubes and fullerenes are similar, we focus here on the major portion of the fusion process. Our search program generates all possible geometries, obtainable by a sequence of generalized Stone-Wales (GSW) bond rearrangements starting from one initial structure, and compares them to the target structure [5]. We restricted our search to GSW transformations [6], which were initially proposed as a general mechanism for the

interconversion between fullerene isomers [7]. The main advantage of the GSW transformations is the low activation barrier, which accelerates the structural transformations in these vacancy-free systems during the zipper closure.

The zipper mechanism of nanotube fusion in the Y-junction geometry, containing one octagon and four heptagons in the junction region, is presented in Fig. 1. Figure 1(a) depicts one transformation cycle from the front view. The detailed bond rearrangements are displayed in Fig. 1(b) as structural diagrams. Each GSW step within the transformation cycle is identified by a rotation of a single bond near the junction of two $(5, 5)$ nanotubes. We emphasize the respective bonds by a thick gray (red) line prior and a thick black line after the rotation. Our results show that a sequence of only nine sequential GSW transformations is sufficient to propagate
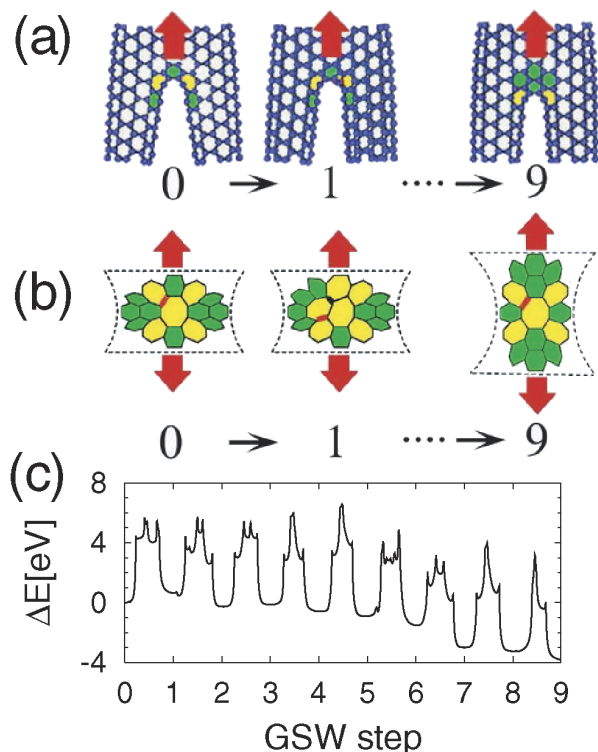

FIG. 1 (color online). Zipper mechanism of the nanotube fusion in the Y-junction geometry of one of our model morphologies, containing one octagon and four heptagons in the junction area. Front view (a) and structural diagrams detailing the bond switching (b), as two $(5, 5)$ nanotubes merge to a $(10, 10)$ nanotube in a morphology reminiscent of pants. The fusion process requires nine generalized Stone-Wales (GSW) transformations to propagate the branching region axially by one period of the armchair nanotube without creating vacancies. Bonds, which are rotated during the individual GSW transformations, are emphasized by thick lines. Details of the complete process are presented at the URL http:// nanotube.msu.edu/ntyjct/. The calculated total energy change ΔE along the minimal energy path connecting the intermediate steps is shown in (c).

the connecting region by one step and thus increase the waist section axially by one period of the $(10, 10)$ nanotube, at the expense of the leg section. In an alternative geometry not discussed here, which contains six heptagons and no higher polygons in the junction region, the axial propagation of the junction by one period can be achieved by only 12 sequential GSW transformations. Following such a full transformation cycle, the final structure (9) is topologically equivalent to the initial structure (0). A related structural transformation, which involves an energetically unstable twelve-membered ring in the junction region, has also been found to provide a pathway to nanotube fusion [8]. There, the GSW sequence has been determined using a "qualitative reasoning assisted search" instead of a computer-assisted complete search. The energetics of the optimized fusion process discussed here, depicted in Fig. 1(c), suggest a monotonic stability increase upon each GSW transformation, in stark contrast to the findings of Ref. [8].

As seen in Fig. 1(c), the fusion process is exothermic. Based on strain energies of infinite structures, we expect an energy gain of 4.8 eV by converting two 0.21 nm long $(5,5)$ nanotube segments to a $(10,10)$ nanotube within one transformation cycle [9]. Total energy calculations for the intermediate structures i, encountered during the fusion process and shown in Fig. 1(c), are performed using the parametrized linear combination of atomic orbitals functional [10] for an $N = 364$-atom cluster representing the structure. All intermediate structures of the system have been fully relaxed using the conjugate gradient technique [11]. Our cluster calculation indicates that the energy is lowered by 4 eV during the complete 9-step transformation cycle, in good agreement with the above 4.8 eV value in view of the finite size of the cluster.

To evaluate the reaction barriers associated with each individual GSW transformation, which play a crucial role in the reaction rate of the zipping process and have not been investigated in Ref. [8], we determine the minimum-energy path in the configuration space using the so-called "string method" [12]. In the string method, the reaction pathway connecting the initial and final N-atom configuration is represented by a string line in the $3N$-dimensional configuration space. In practice, the string is discretized into a sequence of replicas with the constraint of equal arclength between them. The minimum-energy path is found, when the atomic force of every replica along the string is parallel to the tangent of the string. We employ 50 replicas for each GSW step and relax the atomic positions until the normal component of the atomic force becomes less than 0.05 eV/Å in magnitude.

The details of the reaction energy ΔE along the contiguous minimum-energy path, corresponding to the zipper process, are depicted in Fig. 1(c). These results suggest that most GSW transformations are multistep processes with well-defined transition states, as discussed below. We find the maximum energy barrier for a single

GSW step to lie near 5–6 eV. As we discuss in the following, this activated process can proceed relatively fast under the experimental conditions in view of the high rate of subthreshold energy transfer to the structure during electron irradiation [13]. Alternatively, the activation barrier for GSW transformations may be lowered to below 4 eV by autocatalysis reactions [14] involving extra carbon or nitrogen atoms [15]. The 5–6 eV activation energy for the GSW transformation in the Y-junction system lies significantly below the graphene sheet value of ≈ 9 eV based on our approach, or ≈ 8 eV based on *ab initio* calculations [16]. Such a lowering of the activation barrier is expected in nonplanar structures due to the deviation from sp^2 bonding. We find this hypothesis confirmed in our calculations, since lower barriers are found when more heptagons or octagons are closer to the rotating bond.

As mentioned above, we find that most Stone-Wales transformations involve multiple shallow local energy minima, implying a multistep process. These minima originate from local stress release, as two C-C bonds are being broken at the same time as other bonds are being formed during the bond rotation. The barriers surrounding these local minima are very small, suggesting a short lifetime with little effect on the overall reaction rate. In contrast to these findings in the nanotube Y junction, no such local minima occur during the Stone-Wales transformation in graphite due to the absence of tensile stress in that system.

To investigate the effect of high temperatures on the activated fusion process and to identify a possible mechanism that would lower the activation barriers even further, we performed Nosé-Hoover molecular dynamics (MD) calculations at temperatures between 400 and 2400 K. The upper limit of this temperature range is determined by the onset of melting at 2800 K, which starts at the exposed edges of the finite Y-junction or "pants" structure. With increasing temperature, particular vibration modes are stepwise activated. Below 400 K, we observe only local atomic vibrations without global shape changes of the structure. At 800 K, a radial breathing mode of the tubes dominates the dynamics. At 1200 K, the "legs" of the pants structure exhibit a vibration mode, reminiscent of walking and twisting. At 1600 K, this "walking" mode is replaced by a "scissor" mode of the legs, which strains the junction region and lowers the activation barrier for GSW transformations [17]. Snapshots of our molecular dynamics simulation at 1200 K are shown in Figs. 2(a)–2(c).

To obtain independent experimental information about the fusion mechanism, we observed the structural evolution of the nanotube system in an HRTEM. The SWNT samples were generated using either an arc discharge technique involving Ni-Y-graphite electrodes in a He atmosphere [18], or the high-pressure CO conversion (HiPCO) process involving the disproportionation of carbon monoxide over an Fe catalyst [19]. The nanotube
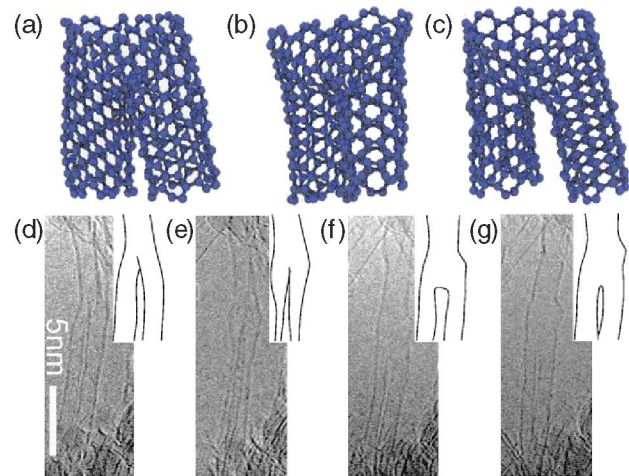

FIG. 2 (color online). Dynamics of partly merged nanotubes. (a)–(c) Snapshots of nanotube pants structures, obtained during a molecular dynamics simulation at $T = 1200$ K, illustrating the excitation of soft vibration modes resembling a walking motion. The corresponding movies are posted at the URL http://nanotube.msu.edu/ntyjct/. (d)–(g) Time sequence of HRTEM images of partially merged SWNTs, where the fusion process was interrupted by an impurity or a chirality difference between the constituent tubes.

material was dispersed ultrasonically in ethanol and deposited onto lacey carbon grids for TEM observations. The experiments were carried out in a high-voltage atomic resolution transmission electron microscope with an accelerating voltage of 1.25 MeV (JEOL-ARM 1250). Observations were performed at specimen temperatures of 800 °C using a Gatan heating stage. Images were recorded with a slow-scan CCD camera. The nanotube behavior was monitored under the electron irradiation corresponding to standard imaging conditions (1.25 MeV electron energy and beam intensity of ≈ 10 A/cm^2).

The time sequence of HRTEM observations in Figs. 2(d)–2(g) provides information about the stability of the nanotube Y junction with respect to electron irradiation and high temperatures. As discussed above, our MD simulations shown Figs. 2(a)–2(c) suggest the occurrence of walking and twisting modes close to 1200 K, the temperature used in the HRTEM observations of Figs. 2(d)–2(g). Figure 2(d) depicts the initial local connection between the tubules, yielding the Y junction. In spite of a subsequent 5-min exposure to electron irradiation, the overall structure appears stable and the shape of the nanotube branches remains essentially the same. The only noticeable change is an overall rotation and twisting of the structure about the axis, as seen in Fig. 2(e). Figure 2(f) provides an optimum view of the junction region, where heptagons and octagons induce a negative Gaussian curvature. During the following 3 min of irradiation, the fusion process continues, but slows down and eventually stops, as shown in Fig. 2(g).

The termination of the fusion process might be due to impurities. Another possible reason is a chirality
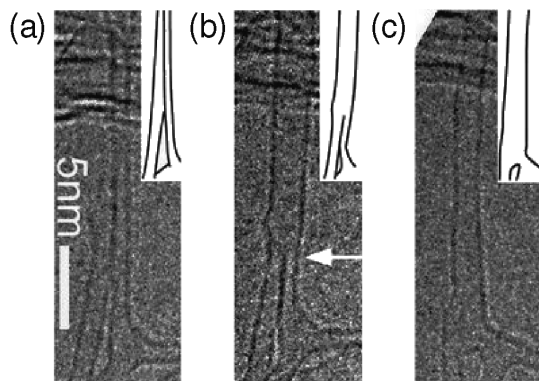
FIG. 3. Time sequence of HRTEM images evidencing the zipper process for the coalescence of two SWNTs. (a) Tubes prior to coalescence at 800 °C. (b) As electron irradiation continues, the nanotubes get closer, overlap, and start merging into one. The fused region is emphasized by the white arrow. (c) The coalescence process is completed, as the fusion region moves down, completing the zipper closure.

mismatch of the tube legs, or the torsion energy required to fuse initially twisted legs, which may be firmly anchored in the substrate. Conceptually, we can imagine one of initially straight tube segments of length L to be cut out first, then twisted by the angle $\Delta\Phi$, and seamlessly reinserted. The resulting average twist of $\Delta\Phi/L$ in the segment comes at a cost in the total torsion energy that is inversely proportional to L. As the constituent tubes continue to merge, thus reducing L while approaching the anchor point, the total strain energy in the twisted tube increases [20]. Independent of the tube stiffness or the initial twist $\Delta\Phi/L$, the strain energy eventually outweighs the energy gain caused by tube fusion. At this point, the fusion process turns endothermic and stops.

In order to study whether nanotubes may merge completely via the zipper mechanism, we have examined two adjacent tubes lying in a plane under electron irradiation at 800 °C. Figures 3(a)–3(c) show a sequence of the zipping process in the pants geometry. In Fig. 3(a), we can distinguish two nanotubes, lying close and parallel to each other. A few minutes later, the tubes were observed to approach even more and started overlapping, as seen in Fig. 3(b). Subsequently, the nanotubes formed a local connection and started merging fast. Figure 3(c) depicts the final stage of this process, a single wide nanotube. The observed fusion process of two tubes into one tubule with a larger diameter, including the intermediate stages and the speed of interconversion, is consistent with our zipper mechanism.

In conclusion, we introduced an energetically efficient microscopic mechanism for nanotube fusion in the Y-junction morphology that requires only GSW bond rotations. Detailed energy calculations revealed that GSW transformations are multistep processes with relatively low activation barriers. Driven by an energy gain, the junction propagates axially, similar to a zipper, in a se-

quence of GSW steps. The propagation of the junction, causing the growth of the fused region, is evidenced in HRTEM observations.

*Permanent address: Department of Physics, Ewha Womans University, Seoul 120-750, Korea.
†Author to whom correspondence should be addressed. Electronic address: tomanek@pa.msu.edu
[1] H. W. Kroto et al., Nature (London) **318**, 162 (1985).
[2] S. Iijima, Nature (London) **354**, 56 (1991).
[3] M. Terrones et al., Science **288**, 1226 (2000).
[4] S. Bandow et al., Chem. Phys. Lett. **337**, 48 (2001).
[5] H. Ueno, S. Osawa, E. Osawa, and K. Takeuchi, Fullerene Sci. Technol. **6**, 319 (1998).
[6] E. Osawa and K. Honda, Fullerene Sci. Technol. **4**, 939 (1996); A. J. Stone and D. J. Wales, Chem. Phys. Lett. **128**, 501 (1986).
[7] P. W. Fowler and D. E. Manolopoulos, *An Atlas of Fullerenes* (Clarendon, Oxford, 1995); E. Osawa et al., J. Chem. Soc. Perkin Trans. **2**, 943 (1998).
[8] Y. F. Zhao, B. I. Yakobson, and R. E. Smalley, Phys. Rev. Lett. **88**, 185501 (2002); Y. F. Zhao, R. E. Smalley, and B. I. Yakobson, Phys. Rev. B **66**, 195409 (2002).
[9] D. Tománek, W. Zhong, and E. Krastev, Phys. Rev. B **48**, 15 461 (1993); D. H. Robertson, D. W. Brenner, and J. W. Mintmire, Phys. Rev. B **45**, 12 592 (1992).
[10] D. Tománek and M. A. Schluter, Phys. Rev. Lett. **67**, 2331 (1991).
[11] W. Press, T. Teukolsky, W. T. Vetterling, and B. P. Flannery, *Numerical Recipes* (Cambridge University Press, Cambridge, England, 1986).
[12] W. E, W. Ren, and E. Vanden-Eijnden, Phys. Rev. B **66**, 052301 (2002).
[13] F. Banhart, Rep. Prog. Phys. **62**, 1181 (1999).
[14] B. R. Eggen et al., Science **272**, 87 (1996).
[15] Z. Slanina et al., J. Organomet. Chem. **599**, 57 (2000).
[16] E. Kaxiras and K. C. Pandey, Phys. Rev. Lett. **61**, 2693 (1988).
[17] M. Buongiorno Nardelli, B. I. Yakobson, and J. Bernholc, Phys. Rev. Lett. **81**, 4656 (1998); Phys. Rev. B **57**, R4277 (1998); P. Zhang, P. E. Lammert, and V. H. Crespi, Phys. Rev. Lett. **81**, 5346 (1998).
[18] C. Journet et al., Nature (London) **388**, 756 (1997).
[19] P. Nikolaev et al., Chem. Phys. Lett. **313**, 91 (1999).
[20] Y.-K. Kwon and D. Tománek, Phys. Rev. Lett. **84**, 1483 (2000).